Photosynth Res (2009) 99:1–10
DOI 10.1007/s11120-008-9346-6

REGULAR PAPER

EPR, ENDOR, and Special TRIPLE measurements of $P^{\bullet+}$ in wild type and modified reaction centers from *Rb. sphaeroides*

J. P. Allen · J. M. Cordova · C. C. Jolley · T. A. Murray · J. W. Schneider · N. W. Woodbury · J. C. Williams · J. Niklas · G. Klihm · M. Reus · W. Lubitz

Received: 29 April 2008 / Accepted: 22 July 2008 / Published online: 26 September 2008

Abstract The influence of the protein environment on the primary electron donor, P, a bacteriochlorophyll *a* dimer, of reaction centers from *Rhodobacter sphaeroides*, has been investigated using electron paramagnetic resonance and electron nuclear double resonance spectroscopy. These techniques were used to probe the effects on P that are due to alteration of three amino acid residues, His L168, Asn L170, and Asn M199. The introduction of Glu at L168, Asp at L170, or Asp at M199 changes the oxidation/reduction midpoint potential of P in a pH-dependent manner (Williams et al. (2001) Biochemistry 40, 15403–15407). For the double mutant His L168 to Glu and Asn at L170 to Asp, excitation results in electron transfer along the A-side branch of cofactors at pH 7.2, but at pH 9.5, a long-lived state involving B-side cofactors is produced (Haffa et al. (2004) J Phys Chem B 108, 4–7). Using electron paramagnetic resonance spectroscopy, the mutants with alterations of each of the three individual residues and a double mutant, with changes at L168 and L170, were found to have increased linewidths of 10.1–11.0 G compared to the linewidth of 9.6 G for wild type. The Special TRIPLE spectra were pH dependent, and at pH 8, the introduction of aspartate at L170 increased the spin density ratio, ρ_L/ρ_M, to 6.1 while an aspartate at the symmetry related position, M199, decreased the ratio to 0.7 compared to the value of 2.1 for wild type. These results indicate that the energy of the two halves of P changes by about 100 meV due to the mutations and are consistent with the interpretation that electrostatic interactions involving these amino acid residues contribute to the switch in pathway of electron transfer.

Keywords Reaction centers · Purple bacteria · Magnetic resonance · Bacteriochlorophyll · Oxidized bacteriochlorophyll dimer · Electron paramagnetic resonance

Abbreviations

EPR	Electron paramagnetic resonance
ENDOR	Electron nuclear double resonance
TRIPLE	Electron-nuclear-nuclear triple resonance
Rb. sphaeroides	*Rhodobacter sphaeroides*
WT	Wild type
RC	Reaction center
P	Primary electron donor
P_L and P_M	L and M sides of P, respectively
BChl	Bacteriochlorophyll
hfc	Hyperfine coupling constant
Q_A	Primary quinone in the RC
Q_B	Secondary quinone in the RC

Introduction

Pigment–protein complexes in photosynthetic organisms convert light energy into chemical energy. In purple

J. P. Allen (✉) · J. M. Cordova · C. C. Jolley · T. A. Murray · J. W. Schneider · N. W. Woodbury · J. C. Williams
Department of Chemistry and Biochemistry and Center for Bioenergy and Photosynthesis, Arizona State University, Tempe, AZ 85287-1604, USA
e-mail: jallen@asu.edu

J. Niklas · G. Klihm · M. Reus · W. Lubitz (✉)
Max-Planck-Institut für Bioanorganische Chemie, Mülheim/Ruhr, Germany
e-mail: lubitz@mpi-muelheim.mpg.de

anoxygenic bacteria, reaction centers (RCs) embedded in the membrane perform the primary photochemistry (Blankenship et al. 1995). The RC from *Rhodobacter sphaeroides* consists of three protein subunits and several cofactors (see e.g., Allen et al. 1987; Yeates et al. 1988; Ermler et al. 1994; Stowell et al. 1997; Camara-Artigas et al. 2002). The core L and M subunits surround the cofactors that are divided into two distinct branches related by an approximate two-fold symmetry axis that runs from the center of P to the non-heme iron (Fig. 1). After light excites the primary electron donor, a bacteriochlorophyll *a* (BChl *a*) dimer, P, an electron is transferred to a series of electron acceptors along the A branch of cofactors and then to the secondary quinone, Q_B, creating the charge-separated state $P^{\bullet+}Q_B^{\bullet-}$. After reduction of $P^{\bullet+}$ by an exogenous cytochrome c_2, P can be excited again, leading to the transfer of a second electron to $Q_B^{\bullet-}$ in a process that is coupled to the uptake of two protons. The generated hydroquinone Q_BH_2 then carries the electrons and protons to the cytochrome bc_1 complex in a cycle that generates the proton gradient needed for the creation of energy-rich compounds.

The two BChls that form P overlap at the ring A position with a separation distance of 3.5 Å (see e.g., Allen et al. 1987; Yeates et al. 1988; Ermler et al. 1994; Stowell et al. 1997). Due to the close contact, the two BChls are electronically coupled and the wavefunction of the unpaired electron is distributed over the conjugated systems of both macrocycles. This has been shown by some of the earliest spectroscopic measurements on the RC, in which a dimeric structure was postulated for the primary donor ("special pair hypothesis")(Norris et al. 1971; 1975; Feher et al. 1975). Electron paramagnetic resonance, EPR, and its advanced multiple resonance methods (ENDOR/TRIPLE) are well-suited for the detailed characterization of the electronic structure of $P^{\bullet+}$ by mapping the spin density distribution over the conjugated system. In wild type, the distribution is asymmetric with more of the spin density being located on the L-side of P (P_L) than the M-side (P_M)(Geßner et al. 1992; Lendzian et al. 1993; Rautter et al. 1994; 1995; 1996; Artz et al. 1997; Müh et al. 2002; Lubitz et al. 2002). Due to the large number of protons in the BChl macrocycle (Fig. 1c) that interact with the unpaired electron of $P^{\bullet+}$, the EPR spectrum shows just a single, unresolved line with a linewidth ΔB_{pp} (peak-to-peak) of 9.6 G (Norris et al. 1971; McElroy et al. 1972; Feher et al. 1975). The linewidth is reduced as compared to that of monomeric BChl $a^{\bullet+}$ ($\sim$14 G at room temperature) due to the dimeric character of $P^{\bullet+}$ (Norris et al. 1971; 1975; McElroy et al. 1972; Feher et al. 1975; Lendzian et al. 1993).

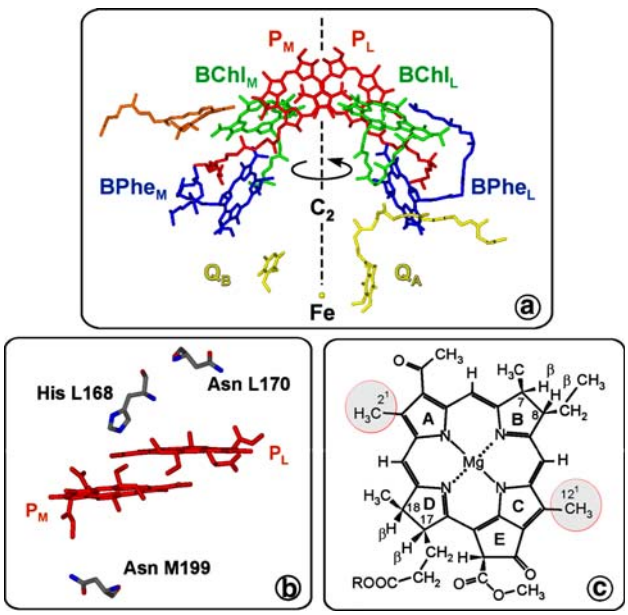

Fig. 1 (**a**) Cofactors in the bacterial photosynthetic RC from *Rb. sphaeroides* (PDB entry 1M3X; Camara-Artigas et al. 2002). (**b**) Structure of the primary donor of the RC from *Rb. sphaeroides* with the two BChl *a* molecules P_L and P_M (phytyl chain truncated), and the three mutated residues His L168, Asn L170, and Asn M199 (PDB entry 1M3X; Camara-Artigas et al. 2002). (**c**) Molecular structure of bacteriochlorophyll *a* (BChl *a*) with IUPAC numbering; the two methyl groups 2^1 and 12^1 and the β-protons 7, 8, 17, and 18 are indicated

Details of the spin density distribution can be obtained by determination of the hyperfine couplings (hfcs) via electron nuclear double resonance, ENDOR (Kurreck et al. 1988; Möbius et al. 1982). If the radical–protein complex rotates fast enough to average out all anisotropic contributions of the hfc (and *g*) tensors only isotropic interactions remain. This results in a single line pair from each set of equivalent protons in the ENDOR spectrum (and a single line in the Special TRIPLE spectrum), which directly yields the isotropic hfcs (Kurreck et al. 1988; Lendzian et al. 1981). It has been shown that for non-aggregated RCs (molecular weight 100 kDa) in detergent containing buffer at 25°C the molecular tumbling is fast enough to average out the *g* anisotropy and all hfc anisotropies of the proton coupling tensors in $P^{\bullet+}$ (Lendzian et al. 1981).

Since ENDOR-in-solution experiments suffer from sensitivity problems (Kurreck et al. 1988; Möbius et al. 1982; Plato et al. 1981), Special TRIPLE is usually used. This technique employs one microwave and two radio frequencies, the latter are symmetrically swept around the nuclear Larmor frequency of the respective nucleus being probed (here ^{1}H). With respect to ENDOR, the method has a higher resolution and is less sensitive to the balance of electron and nuclear relaxation rates (Kurreck et al. 1988; Möbius et al. 1982; Plato et al. 1981). For these reasons, Special TRIPLE has a significant advantage when investigating $P^{\bullet+}$, which gives a weak signal and provides congested spectra. In a series of ENDOR and TRIPLE

studies of $P^{\bullet+}$ in RCs both in liquid solution and single crystals, several hfcs have been resolved and unambiguously assigned (Geßner et al. 1992; Lendzian et al. 1993; Artz et al. 1997; Rautter et al. 1994; 1995; 1996; Müh et al. 2002). In general, for samples in liquid solutions, the technique of Special TRIPLE is well suited to obtain high-quality spectra that can be used to gain detailed insight into the spin and charge distribution within $P^{\bullet+}$. These techniques have also been used to investigate the effect of a number of different mutations in bacterial photosynthetic RCs (Artz et al. 1997; Rautter et al. 1995; 1996; Müh et al. 1998; 2002; Lubitz et al. 2002).

In general, the surrounding protein environment has been found to play a critical role in determining the properties of the electronic states of P (Allen and Williams 2006; Williams and Allen 2008). In wild type, there is one hydrogen bond between His L168 and the acetyl group of ring A (P_L) (Fig. 1b). Mutants with the number of hydrogen bonds to the conjugated system of P ranging from zero to four have midpoint potentials from 410 to 765 mV, compared to 505 mV for wild type (Lin et al. 1994). These mutants also show significant shifts in the spin density distribution over the two halves of P (Rautter et al. 1995; Artz et al. 1997; Müh et al. 2002). The shifts of the $P/P^{\bullet+}$ midpoint potential and spin density are correlated and provided the basis for detailed theoretical models of the electronic structure of $P^{\bullet+}$ (Müh et al. 2002; Reimers and Hush 2003; 2004).

In addition to hydrogen bonds, electrostatic interactions have been shown to influence the energy of $P^{\bullet+}$. These interactions have been probed by insertion or removal of ionizable residues at several different residue positions located ~10–15 Å from the primary donor (Williams et al. 2001; Johnson and Parson 2002; Johnson et al. 2002). Several of the mutants showed a pronounced effect on the $P/P^{\bullet+}$ midpoint potential and thus also on the primary electron transfer (Williams et al. 2001; Haffa et al. 2002; 2003; 2004). The amino acid residue Asn M199 is located 8.5 Å from P (this is the closest distance from the oxygen or nitrogen atoms of the side chain to the conjugated atoms of P) (Fig. 1b). At pH 8, substitution of Asn M199 with Asp in the ND(M199) mutant was found to result in a 48-mV decrease in the midpoint potential compared to wild type. The replacement of Asn L170, which is located at a comparable distance on the symmetry related side (Fig. 1b), with Asp in the ND(L170) mutant resulted in a 44-mV lowering of the midpoint potential at pH 8 compared to wild type while a 75-mV decrease was observed for the mutation of His L168, which is hydrogen-bonded to the acetyl group of P_L, to Glu in the HE(L168) mutant. The effect of having two alterations, His L168 to Glu and Asn L170 to Asp in the HE(L168)/ND(L170) mutant, was more pronounced with a decrease of 127 mV in the midpoint potential. The $P/P^{\bullet+}$ midpoint potential was found to be pH dependent in these mutants. For example, the $P/P^{\bullet+}$ midpoint potential for the ND(M199) mutant decreased by 53 mV as the pH was increased from 6.0 to 9.5 (Williams et al. 2001). The mutants were found to have initial electron transfer times ranging from 1.8 to 2.9 ps compared to 3.1 ps for wild type at pH 8 (Haffa et al. 2002). Use of 850 nm light to directly excite P resulted in formation of the charge-separated state $P^{\bullet+}Q_A^{\bullet-}$ in all mutants. However, use of light at shorter wavelengths of 390, 740, or 800 nm, produced a long-lived charge-separated state consisting of the oxidized M-side BChl and reduced M-side bacteriopheophytin, $B_B^{\bullet+}H_B^{\bullet-}$, rather than a state involving $P^{\bullet+}$(Haffa et al. 2003). For the HE(L168)/ND(L170) double mutant, initial electron transfer following 390 nm excitation was strongly pH dependent, with primarily A-side transfer at pH 7.2 but formation of the $B_B^{\bullet+}H_B^{\bullet-}$ state dominating at pH 9.5 (Haffa et al. 2004). In this work, the effect of the electrostatic interactions on the properties of $P/P^{\bullet+}$ in these mutants is investigated by EPR and ENDOR/TRIPLE measurements.

Materials and methods

Rhodobacter sphaeroides wild type 2.4.1 was grown under photosynthetic conditions. The RCs isolated from these cells were purified as previously described (van Mourik et al. 2001).

Cultures of *Rb. sphaeroides* wild type containing a hepta-histidine tag (WT-H7) and the four mutants, ND(L170), HE(L168), ND(M199), and HE(L168)/ND(L170), were grown under non-photosynthetic conditions (Williams et al. 2001). For isolation of these RCs, a hepta-histidine tag at the carboxyl terminal region of the M-subunit was used as described previously (Goldsmith and Boxer 1996). After purification, the RCs were placed in 15 mM tris(hydroxymethyl)-aminomethane pH 8, 0.025% lauryl dimethylamine oxide, and 1 mM EDTA. Before measurement, the samples were either kept in this buffer (for measurements at pH 8.0) or exchanged by repetitive concentration/dilution using 30 kDa Centricon or Microcon filters into 2-(*N*-morpholino)ethanesulfonic acid (MES) pH 6.5 or (2-[*N*-cyclohexylamino]ethane sulfonic acid (CHES) pH 9.5. Finally, the samples were concentrated to an OD_{802} of 80–130.

CW X-band EPR measurements were performed with a Bruker ESP 300 spectrometer at room temperature using a rectangular cavity with optical access (TE_{102}, ER 4102ST, Bruker), using a capillary with 1 mm inner diameter. The radical cation $P^{\bullet+}$ was created via continuous illumination with white light in situ, using heat-absorbing glass and water filters.

CW X-band Special TRIPLE measurements were done on the same spectrometer at 288 K. A home-built ENDOR cavity was used, similar to the one previously described

(Zweygart et al. 1994), but with a nitrogen gas cooling system. The cation radical $P^{\bullet+}$ was created in situ as described above. The data analysis was performed using home-written routines in Matlab^{TM}, similar to the program used before (Tränkle and Lendzian 1989). In several cases, a baseline was recorded under identical conditions (with the magnetic field off-resonant and subtracted) under the assumption that possible drifts and artifacts would be the same in both cases.

Q-band EPR and ENDOR measurements in frozen solution were done on a Bruker Elexsys E580 spectrometer at 80 K. For frozen solution experiments, sucrose (60%) was added to all samples. A home-built resonator was used (Silakov et al. 2007), similar to the one described previously (Sienkiewicz et al. 1996). A Davies-type pulse ENDOR experiment (Davies 1974) was performed as described previously (Epel et al. 2006).

Results

X-band EPR measurements

Measurements using the X-band EPR spectrometer were performed for both wild-type RCs and the four mutants, ND(L170), HE(L168), ND(M199), and HE(L168)/ND(L170), in liquid solution. In all cases, the spectrum was a single unresolved line centered at g close to g_e (see Fig. 2 for an example).

For wild-type RCs at pH 8.0, the spectrum was simulated using a Gaussian function with a linewidth ΔB_{pp} (peak-to-peak) of 9.6 G (±0.2 G) at $g = 2.0026$ in agreement with published data of this radical in RCs from *Rb. sphaeroides* 2.4.1 (see for example Feher et al. 1975; Norris et al. 1971; Artz et al. 1997). The spectrum of the four mutant RCs at pH 8.0 were fitted yielding the same g-value and different Gaussian linewidths. For all of the mutants, the EPR linewidth was increased relative to wild type. The linewidth is smallest for the ND(M199) mutant (10.1 G), followed by the HE(L168) mutant (10.2 G), with the ND(L170) mutant and the double mutant HE(L168)/ND(L170) having the most pronounced increase (11.0 G). The increase in linewidth for the mutants indicates a stronger asymmetry of the dimer than found for wild type (Lendzian et al. 1993). However, the mutations may also cause local effects like spin redistributions within the BChl macrocycles or change the geometry of the BChl macrocycles. Since the hfcs of the β-protons at positions 7, 8, 17, and 18 (Fig. 1c) are strongly dependent on the geometry of the respective hydrated rings (Rautter et al. 1995), the EPR linewidth may be changed even without a spin redistribution between the two halves of the dimer. More definitive conclusions can, therefore, only be drawn if the resolution is increased significantly, e.g., by double and triple resonance experiments, yielding the individual nuclear hyperfine coupling constants.

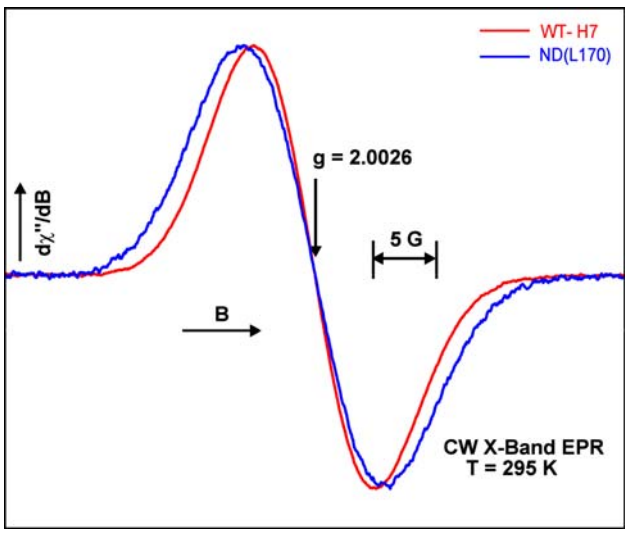

Fig. 2 Comparison of CW X-band EPR spectra of light-induced $P^{\bullet+}$ in RCs from *Rb. sphaeroides* wild type with hepta-histidine tag (WT-H7) (red line) and from ND(L170) (blue line) at pH 8.0

X-band CW ^{1}H Special TRIPLE measurements

$P^{\bullet+}$ in Wild-Type RCs

Figure 3 compares the Special TRIPLE spectra of WT 2.4.1 (bacteria grown photosynthetically) and WT-H7 (hepta-histidine tag, grown non-photosynthetically) at pH 8.0. The WT 2.4.1 spectrum is identical to that observed before (Geßner et al. 1992; Artz et al. 1997; Müh et al. 2002). The assignment of lines and hfcs (Table 1) follows that of our earlier work (Geßner et al. 1992; Lendzian et al. 1993). Most pronounced are the resonances of the protons of the four (freely rotating) methyl groups (positive hfcs)[1] and the two β-protons (L-side, positive hfcs). As an indicator for the spin density distribution in the BChl macrocycle, the hfcs of the β-protons at the positions 7, 8, 17, and 18 are less suited, since they are sensitive to the dihedral angle of the respective rings that can easily change (Käss et al. 1994; Rautter et al. 1995). The two spectra show some very small but distinct differences of the proton hfcs. Based upon previous studies, the shifts are unlikely to arise from a difference in the carotenoid composition, due to incorporation of spheroidene and spheroidenone in

[1] Methyl groups: attached to the conjugated π-system. Due to the fast rotation, the three protons are magnetically equivalent. β-protons: Protons not directly attached to the conjugated π-system, not belonging to methyl groups, see Fig. 1.

cultures grown under anaerobic and aerobic conditions, respectively, or differences in the preparations (Geßner et al. 1992; Rautter et al. 1994). The ENDOR/TRIPLE spectrum is sensitive to electrostatic interactions as indicated by the large changes observed upon introduction of hydrogen bonds or use of zwitterionic detergents (Rautter et al. 1995; Müh et al. 1998; 2002). Thus, the most likely cause for the small spectral shift is addition of electrostatic interactions due to the presence of the hepta-histidine tag at the carboxyl terminus region of the M-subunit. For the discussion concerning the mutants, since the changes are very small, the two wild-type samples can be considered to be basically equivalent.

$P^{\bullet+}$ *in mutant RCs*

Since the mutants show pronounced pH dependences of the $P/P^{\bullet+}$ midpoint potential and electron transfer rates, the spectra were measured at three different pH values, 6.5, 8.0, and 9.5. The wild type showed no spectral changes at the pH values of 8.0 and 9.5. Differences in the spectra of the mutants compared to wild type should be predominately due to the substitution of the amino acid residue, excluding any spatial structural changes of $P/P^{\bullet+}$. Based upon previous studies (Haffa et al. 2002; 2003; 2004; Williams et al. 2001), comparison of the spectra of the mutants at different pH values should show the effect of changes in the protonation, or charge, of the introduced residue. At any given pH, the deprotonated and protonated

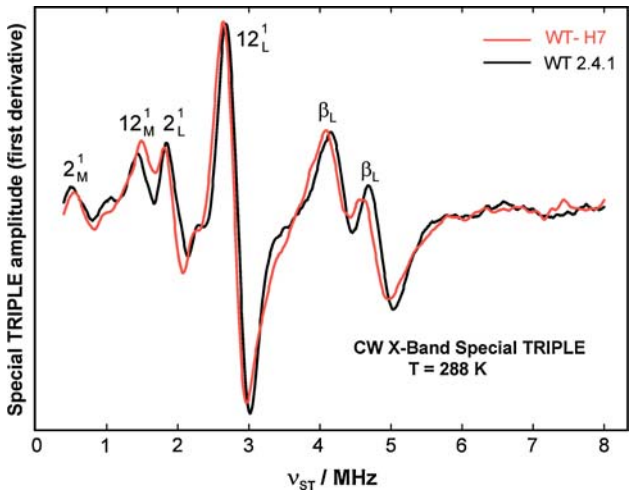

Fig. 3 ^{1}H-Special TRIPLE spectra (X-band) of light-induced $P^{\bullet+}$ from RCs from *Rb. sphaeroides* wild type 2.4.1 (WT 2.4.1) (black line) and from wild type with hepta-histidine tag (WT-H7) (red line) at pH 8.0. The isotropic hyperfine couplings a_{iso} are directly obtained from the Special TRIPLE frequency by $\nu_{ST} = a_{iso}/2$ (for details see Lendzian et al. 1993). Assignments of the lines to molecular positions of the L- and the M-half of the BChl-dimer are given (cf. structure in Fig. 1c)

Table 1 ^{1}H hfcs [MHz] of $P^{\bullet+}$ in wild-type reaction centers from *Rb. sphaeroides* and mutants at pH 8.0 with (tentative) assignments, ratios and sums of hfcs, and EPR linewidths

	Wild type[a]	Wild type[b]	ND(L170)	ND(M199)
$A(12^1_L)$	5.64	5.57 [5.43]	6.82 [7.00]	3.54
$A(2^1_L)$	4.01	3.90 [3.86]	4.98	2.59
$A(12^1_M)$	3.10	3.21	~1.4	6.32
$A(2^1_M)$	1.36	1.30	~0.58 (calc.)	2.59
β_L (strong)	9.70/8.66	9.51/8.52	13.28/11.52	
β_M (strong)				12.61/11.24
$A(12^1_L)/A(2^1_L)$	1.41	1.43	1.37	1.37
$A(12^1_M)/A(2^1_M)$	2.28	2.47	2.4(from WT)	2.44
ΣA	14.11	13.98	~13.78	15.04
ρ_L	0.68	0.68	~0.86	0.41
ρ_L/ρ_M	2.13	2.13	~6.14	0.69
ΔBpp [G]	9.6	9.6	11.0	10.1

[a] Wild type *Rb. sphaeroides* 2.4.1 grown under photosynthetic conditions

[b] Wild type *Rb. sphaeroides* with hepta-histidine tag (WT-H7) grown under non-photosynthetic conditions

ΔBpp [G] is the peak-to-peak gaussian envelope EPR line width; the error is ±0.2 G

Error for methyl group hfcs is ±70 kHz, for other β-proton hfcs ±120 kHz, for the double mutant the errors are higher

a_{iso} values given in square brackets are from frozen solution Q-band ENDOR experiments

ΣA is the sum of $A(12^1_L)$, $A(2^1_L)$, $A(12^1_M)$, and $A(2^1_M)$

ρ_L is the fraction of spin density on ρ_L as measured by $[A(12^1_L) + A(2^1_L)]/[A(12^1_L) + A(2^1_L) + A(12^1_M) + A(2^1_M)]$

ρ_L/ρ_M is the ratio of the spin densities on P_L and P_M as measured by $[A(12^1_L) + A(2^1_L)]/[A(12^1_M) + A(2^1_M)]$

forms of the residue will be in equilibrium with a ratio determined by the pK_a value. If the protonation and deprotonation process is fast compared to the EPR/TRIPLE timescale, only an averaged single species with a shifted spin density distribution will be observed. If the protonation and deprotonation process is slower, two different species associated probably with different spectral properties are expected. Considering that already the Special TRIPLE spectra of one species is rather complicated due to the large number of coupled protons, it becomes difficult to disentangle these spectra containing contributions from two $P^{\bullet+}$ species. Upon a pH change, either the magnitude of the hfcs will change (L-side and M-side hfcs in opposite direction) or the portion of one species will increase while the other one will decrease.

The assignment of the hfcs in $P^{\bullet+}$ spectra of mutant RCs has been greatly aided by determining the magnitudes of the four large methyl hfcs, two from each side of the dimer (P_L and P_M). We have previously measured and analyzed a large number of mutant RCs (Rautter et al. 1995; 1996;

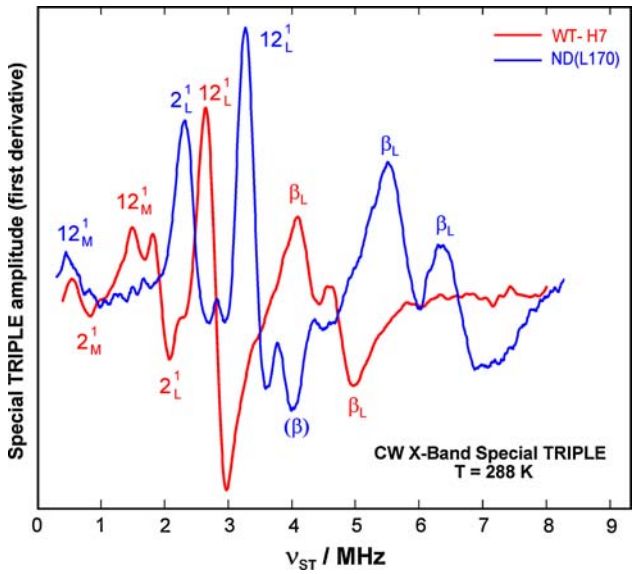

Fig. 4 ^{1}H-Special TRIPLE spectra (X-band) of light-induced $P^{\bullet+}$ from RCs from *Rb. sphaeroides* wild type with hepta-histidine tag (WT-H7) (red line) and from the mutant ND(L170) (blue line) at pH 8.0. The isotropic hyperfine couplings a_{iso} are directly obtained from the Special TRIPLE frequency by $\nu_{ST} = a_{iso}/2$ (for details see Lendzian et al. 1993). Assignments of the lines to molecular positions of the L- and the M-half of the BChl-dimer are given (cf. structure in Fig. 1c)

Artz et al. 1997; Müh et al. 2002; Lubitz et al. 2002) and the ratio between these hfcs on the respective halves has always been similar, except for mutations that lead to rotation of the acetyl groups of P. In addition, the sum of these four hfcs was found to be constant at ~14 MHz. The spectra of the four mutants are discussed individually below. For the ND(L170) and ND(M199) mutants the respective hfcs are given in Table 1.[2]

ND(L170) mutant The Special TRIPLE spectrum of ND(L170) RCs at pH 8.0 is shown in Fig. 4 in comparison with the spectrum of WT-H7 at pH 8.0. The $P^{\bullet+}$ spectrum of the mutant RCs shows two intense, well-resolved signals from β-proton hfcs that are much larger than those in wild type with the two largest methyl group hfcs also larger than found in wild type. Since the ratio between these methyl group hfcs is 1.37, which is typical for the two methyl groups on P_L, the strongly coupled β-protons must belong to the L-side, too. In addition, there are several less intense signals overlapping with the methyl groups that are probably due to β-protons. A broader peak around 1.4 MHz is observed that probably arises from several protons, including the stronger coupled methyl group of the M-side. The smaller methyl group is expected to be ~2.4 times smaller and is out of our detection range.

[2] Some of the mutants were more sensitive than wild type resulting in degradation, which limited the signal-to-noise ratio of the spectra.

The spectrum from this mutant at pH 8.0 looks very different from that of wild type and resembles the spectra of the heterodimer mutants. In the heterodimer mutants, the exchange of His L173, which coordinates the central Mg of P_M, to Leu results in the incorporation of bacteriopheophytin in place of P_M (Bylina and Youvan 1988) with most of the spin density being located on P_L (Nabedryk et al. 2000; Schulz et al. 1998; Rautter et al. 1995). Hence, it has to be concluded that in $P^{\bullet+}$ of ND(L170) RCs most of the spin density (86%) is located on P_L, which is attributed to the presence of the charged Asp at position L170. Similar electrostatic effects have been reported earlier for mutant RCs (Johnson et al. 2002). An increase of the pH to 9.5 did not alter the spectrum very much (data not shown). If we assume that the residue is completely deprotonated, the pK_a should be under 8.0. At pH 6.5, the RCs became unstable and no spectra could be obtained.

ND(M199) mutant The Special TRIPLE spectra of ND(M199) RCs at pH 6.5, 8.0, and 9.5 are shown in Fig. 5. At pH 8.0, the two large β-proton hfcs are shifted to higher values compared to wild type and a third strongly coupled β-proton is visible. Four intense and narrow lines are present that are assigned to methyl groups. Assuming both larger methyl hfcs belong to the L-side and the two smaller hfcs to the M-side, ratios of 1.79 and 1.57 are calculated, respectively, which are both very different from the values of 2.4 and 1.4 found for wild type and most mutants

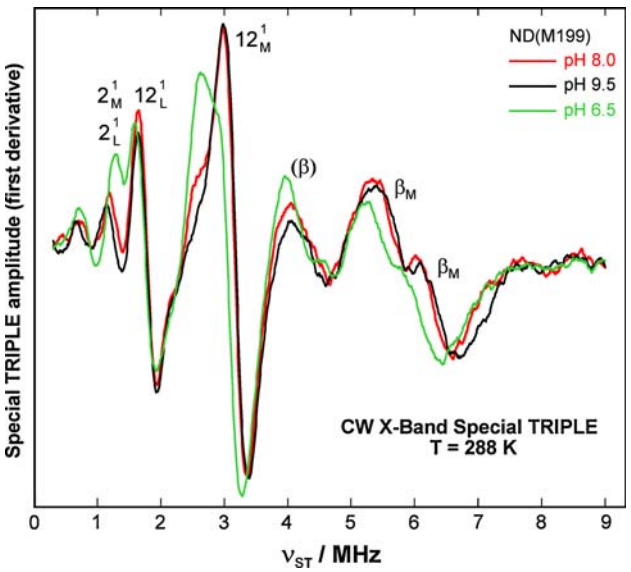

Fig. 5 ^{1}H-Special TRIPLE spectra (X-band) of light-induced $P^{\bullet+}$ from RCs from *Rb. sphaeroides* mutant ND(M199) at pH 6.5 (green), 8.0 (red), and 9.5 (black). The isotropic hyperfine couplings a_{iso} are directly obtained from the Special TRIPLE frequency by $\nu_{ST} = a_{iso}/2$ (for details see Lendzian et al. 1993). Assignments of the lines to molecular positions of the L- and the M-half of the BChl-dimer are given (cf. structure in Fig. 1c)

(Rautter et al. 1995). However, an assignment of the hfcs with 6.32 and 2.59 MHz to one side yields a ratio of 2.44 that would fit very nicely to the M-side but the remaining two lines yield a ratio of 2.18 that does not fit to the L-side at all. The assumption that the signal at 2.59 MHz represents an overlap of L-side and M-side methyl hfcs signals solves this problem, as the ratio of 3.54/2.59 is equal to 1.37, which is the expected ratio for the L-side (Table 1). This assumption leaves the smallest signal of 1.62 MHz unassigned.

The pH dependence for the $P/P^{\bullet+}$ midpoint potential of this mutant between pH 6.5 and 9.5 was well described using the Henderson–Hasselbalch equation with a pK_a of 7.9 (Williams et al. 2001). Consequently, we can expect at pH 8.0 a contribution of two different species, one protonated and the other deprotonated (if the rate constants are slower than the time resolution of the TRIPLE experiment, see discussion above). Comparison with the spectra at pH 9.5 and 6.5 shows that some lines change intensity. This pH difference seems to indicate the presence of two species that could be associated with the protonated and the deprotonated state of the Asp residue. The high pH form (deprotonated) has more spin density on P_M and the low pH form (protonated) is similar to wild type with a dominant P_L spin density. A species with several lines similar to those of wild type can indeed be found in the spectrum of this mutant at pH 6.5 (already present with lower intensity at pH 8.0) (see Fig. 5).

HE(L168) and HE(L168)/ND(L170) mutants Special TRIPLE spectra of HE(L168) RCs were recorded at pH 8.0 and 6.5 (data not shown). In comparison to wild-type, the spectrum at pH 8.0 is changed with regard to the signals of the β-protons and the methyl group protons. His L168 forms a hydrogen bond to the oxygen of the acetyl group at position 3 in the BChl macrocycle of the L-side. Hence, the mutation may alter the hydrogen bonding and the acetyl group may undergo a change in its orientation. This leads not only to a shift of spin density between the two halves of P but also results in a redistribution of the spin density within the BChl macrocycle (Rautter et al. 1995). Previous measurements of the spectrum of the mutant HF(L168) were interpreted with the dimer becoming nearly symmetric with slightly more spin density (57%) on the P_M half of the dimer. In addition, it cannot be excluded that protonated glutamic acid at lower pH may form a hydrogen bond in contrast to its deprotonated form. The RCs of the double mutant HE(L168)/ND(L170) could be measured only at pH 8.0 (data not shown) due to degradation of the sample at other pH values that seriously limited the signal-to-noise. The problems with the assignment discussed for the mutant HE(L168) apply here, too. Due to these different possible influences and the limited quality of the spectra, no assignments have been made for either of these mutants and they are not discussed below.

Pulsed Q band ENDOR measurements

Experiments in frozen solution of wild type and mutant RCs were performed in addition to liquid solution with the aim of corroborating the hfc data. The advantage of frozen solution is better sample stability and larger sample volume leading to better intensities. In frozen solution, all anisotropic contributions are no longer averaged out. Frozen solution ENDOR thus delivers additional information, but the resolution is strongly decreased in these spectra. Due to their small anisotropy, the methyl groups give fairly strong and narrow signals in such spectra. In wild type, only the two methyl groups with the largest couplings could be simulated, and in the mutants studied in this work only the one with the largest methyl hfc. The deduced isotropic hfcs (Table 1) are the same as those obtained from liquid solution experiments within error. Thus, the frozen ENDOR measurements fully support our Special TRIPLE measurements in the liquid state.

Discussion

In earlier work, it has been shown that the spin density distribution of the primary donor radical cation $P^{\bullet+}$ in bacterial RCs is a very sensitive probe for structural and electrostatic changes of the dimer and its surrounding. The spin density shifts have for example been correlated with the redox potential of $P/P^{\bullet+}$ and the electron transfer rates (Rautter et al. 1996; Müh et al. 2002; Lubitz et al. 2002). In the present work, it was shown that even a His-tag attached to the RC leads to a small change of the $P^{\bullet+}$ characteristics. In the mutants, the effects are much larger.

Two of the mutants, ND(L170) and ND(M199), are located at symmetry related locations that are $\sim$8.5 Å away from P (Fig. 1b). The effects of these mutations should be primarily electrostatic, with the non-protonated form (charged Asp residue) being predominant at high pH (Williams et al. 2001). For ND(L170), the spin density was found to be shifted to the L-side (86% on P_L) compared to 68% for wild type. In the case of ND(M199), the spin density was shifted in the opposite direction with only 41% of the spin being on the L-side of P. For the ND(M199) mutant, the ratios of the methyl group hfcs and the pH dependence are reasonable if we assume that the signal at 2.59 MHz arises from two methyl groups. In these spectra, lines from a second species are evident with different intensities at different pH values. These spectral differences indicate a pH-dependent equilibrium between two species with a pK_a value close to 8 as found in

measurements of the pH dependence of the $P/P^{\bullet+}$ midpoint potential (Williams et al. 2001).

Such behavior is consistent with the energies of P shifting in response to charges on these two amino acid residues. A negatively charged residue on M199 should destabilize P_M, and hence make the two halves more symmetric resulting in a decrease in the spin density on P_L. Likewise, a negatively charged residue on L170 should destabilize the energy of P_L making the two halves more asymmetrical resulting in an increase of the spin density on P_L. These effects are opposite to those observed for the hydrogen bonding mutants (Artz et al. 1997; Rautter et al. 1995; 1996; Müh et al. 2002; Lubitz et al. 2002), as the introduction of a hydrogen bond to the conjugated system of P can be thought of as introducing a net partial positive charge.

The changes in spin density distribution can be directly related to the change in the energy of one of the BChls (Müh et al. 2002). The spin-density ratios, ρ_L/ρ_M, are 6.1 and 0.7 for ND(L170) and ND(M199), respectively, compared to 2.1 for wild type. These ratios correspond to energy differences between P_L and P_M of +150 and −45 meV for ND(L170) and ND(M199), respectively, as compared to +60 meV for wild type. Thus, the two mutations both increase the energy of the nearest cofactor, P_L for ND(L170) and P_M for ND(M199), by nearly the same amount of 90 and 105 meV, respectively. Since in both cases the energy of P_L or P_M is increasing, the midpoint potential should decrease. For the ND(M199) mutant, the midpoint potential was measured to decrease by 73 mV relative to wild type at pH 9.5, where Asp M199 is expected to be fully ionized (Williams et al. 2001). The extent of the midpoint potential is comparable but not exactly matching the predicted relationship based upon the hydrogen bonding mutants (Müh et al. 2002; Reimers and Hush 2003; 2004). By comparison, spin density ratios of 3.1 and 1.6 were observed for mutants in which Arg was replaced with Glu at the symmetry related positions L135 and M164, respectively (Johnson et al. 2002). For the L135 and M164 mutants, the changes in energy of P_L and P_M are smaller than those observed for L170 and M199, indicating that the electrostatic interactions are dependent on the distance and orientation relative to P. The results from the mutations at these four residues show that the energies of P_L or P_M can be preferentially changed depending on the placement of a charged residue.

The amount of B-side electron transfer after excitation at 390 nm has been observed to be altered in the HE(L168)/ND(L170) mutant in a pH-dependent manner that has been interpreted as arising from the presence of ionizable amino acids residues (Haffa et al. 2004). At pH 7.2, electron transfer occurs along the A-branch resulting in the charge-separated state $P^{\bullet+}Q_A^{\bullet-}$. At pH 9.5, excitation leads to electron transfer involving the B branch of cofactors and results in the state $B_B^{\bullet+}$ $H_B^{\bullet-}$. The present ENDOR/TRIPLE measurements are consistent with the proposal that the switch to B-side electron transfer is due to electrostatic interactions involving the cofactors and the introduced substitutions. The results indicate that the energies of P_L and P_M change by about 100 meV due to these charges. The comparable distances of L170 to P and B_B, 9.0 and 10.5 Å respectively, suggests that B-side electron transfer occurs at least partially by a decrease of the energy of $B_B^{\bullet+}$ by 100 meV, thus favoring formation of $B_B^{\bullet+}$ $H_B^{\bullet-}$ (Haffa et al. 2004). In general, these data are not only consistent with the idea that B-side electron transfer can be manipulated by the introduction of charges that favor formation of the B-side charge-separated states but also provide a means to quantify the energies of these states.

Acknowledgments Student support for this project was provided by the ASU's IGERT in Biomolecular Nanotechnology, funded by the NSF (DGE-0114434). As part of this project, students were able to prepare samples at ASU and spend time performing research in Mülheim/Ruhr. In addition, students also performed FTIR measurements in Saclay with Eliane Nabedryk and Jacques Breton; we gratefully acknowledge their hospitality during this work. Alexey Silakov (MPI Mülheim) is acknowledged for writing the Matlab routine to analyze the Special TRIPLE spectra. The work was partially supported from the NSF (MCB0640002 and MCB0642260) and from the Max Planck Society.

References

Allen JP, Williams JC (2006) The influence of protein interactions on the properties of the bacteriochlorophyll dimer in reaction centers. In: Grimm B, Porra RJ, Rüdiger W, Scheer H (eds) Chlorophylls and bacteriochlorophylls: biochemistry, biophysics functions and applications. Springer, Dordrecht, pp 283–295

Allen JP, Feher G, Yeates TO, Komiya H, Rees DC (1987) Structure of the reaction center from *Rhodobacter sphaeroides* R-26: the cofactors. Proc Natl Acad Sci USA 84:5730–5734

Allen JP, Artz K, Lin X, Williams JC, Ivancich A, Albouy D, Mattioli TA, Fetsch A, Kuhn M, Lubitz W (1996) Effects of hydrogen bonding to a bacteriochlorophyll–bacteriopheophytin dimer in reaction centers from *Rhodobacter sphaeroides*. Biochemistry 35:6612–6619

Artz K, Williams JC, Allen JP, Lendzian F, Rautter J, Lubitz W (1997) Relationship between the oxidation potential and electron spin density of the primary electron donor in reaction centers from *Rhodobacter sphaeroides*. Proc Natl Acad Sci USA 94:13582–13587

Blankenship RE, Madigan MT, Bauer CE (eds) (1995) Anoxygenic photosynthetic bacteria. Kluwer Academic Publishers, Dordrecht

Bylina EJ, Youvan DC (1988) Directed mutations affecting spectroscopic and electron transfer properties of the primary donor in the photosynthetic reaction center. Proc Natl Acad Sci USA 85:7226–7230

Camara-Artigas A, Brune D, Allen JP (2002) Interactions between lipids and bacterial reaction centers determined by protein crystallography. Proc Natl Acad Sci USA 99:11055–11060

Davies ER (1974) A new pulse ENDOR technique. Phys Lett A 47: 1–2

Epel B, Niklas J, Sinnecker S, Zimmermann H, Lubitz W (2006) Phylloquinone and related radical anions studied by pulse electron nuclear double resonance spectroscopy at 34 GHz and density functional theory. J Phys Chem B 110:11549–11560

Ermler U, Fritzsch G, Buchanan SK, Michel H (1994) Structure of the photosynthetic reaction centre from *Rhodobacter sphaeroides* at 2.65 Å resolution: cofactors and protein-cofactor interactions. Structure 2:925–936

Feher G, Hoff AJ, Isaacson RA, Ackerson LC (1975) ENDOR experiments on chlorophyll and bacteriochlorophyll in vitro and in the photosynthetic unit. Ann NY Acad Sci 244:239–259

Geßner C, Lendzian F, Bönigk B, Plato M, Möbius K, Lubitz W (1992) Proton ENDOR and TRIPLE resonance investigation of $P_{865}^{\bullet+}$ in photosynthetic reaction center single crystals of *Rb. sphaeroides* wild type 2.4.1. Appl Magn Res 3:763–777

Goldsmith JO, Boxer SG (1996) Rapid isolation of bacterial photosynthetic reaction centers with an engineered poly-histidine tag. Biochim Biophys Acta 1276:171–175

Haffa ALM, Lin S, Katilius E, Williams JC, Taguchi AKW, Allen JP, Woodbury NW (2002) The dependence of the initial electron-transfer rate on driving force in *Rhodobacter sphaeroides* reaction centers. J Phys Chem B 106:7376–7384

Haffa ALM, Lin S, Williams JC, Taguchi AKW, Allen JP, Woodbury NW (2003) High yield of long-lived B-side charge separation at room temperature in mutant bacterial reaction centers. J Phys Chem B 107:12503–12510

Haffa ALM, Lin S, Williams JC, Bowen BP, Taguchi AKW, Allen JP, Woodbury NW (2004) Controlling the pathway of photosynthetic charge separation in bacterial reaction centers. J Phys Chem B 108:4–7

Johnson ET, Parson WW (2002) Electrostatic interactions in an integral membrane protein. Biochemistry 41:6483–6494

Johnson ET, Müh F, Nabedryk E, Williams JC, Allen JP, Lubitz W, Breton J, Parson WW (2002) Electronic and vibronic coupling of the special pair of bacteriochlorophylls in photosynthetic reaction centers from wild-type and mutant strains of *Rhodobacter sphaeroides*. J Phys Chem B 106:11859–11869

Käss H, Rautter J, Zweygart W, Struck A, Scheer H, Lubitz W (1994) EPR, ENDOR, and TRIPLE-resonance studies of modified bacteriochlorophyll cation radicals. J Phys Chem 98:354–363

Kurreck H, Kirste B, Lubitz W (1988) Electron nuclear double resonance spectroscopy of radicals in solution—applications to organic and biological chemistry. VCH Publishers, Deerfield Beach, FL

Lendzian F, Lubitz W, Scheer H, Bubenzer C, Möbius K (1981) In vivo liquid solution ENDOR and TRIPLE resonance of bacterial photosynthetic reaction centers of *Rhodopseudomonas sphaeroides* R-26. J Am Chem Soc 103:4635–4637

Lendzian F, Huber M, Isaacson RA, Endeward B, Plato M, Bönigk B, Möbius K, Lubitz W, Feher G (1993) The electronic structure of the primary donor cation radical in *Rhodobacter sphaeroides* R-26: ENDOR and TRIPLE resonance studies in single crystals of reaction centers. Biochim Biophys Acta 1183:139–160

Lin X, Murchison HA, Nagarajan V, Parson WW, Allen JP, Williams JC (1994) Specific alteration of the oxidation potential of the electron donor in reaction centers from *Rhodobacter sphaeroides*. Proc Natl Acad Sci USA 91:10265–10269

Lubitz W, Lendzian F, Bittl R (2002) Radicals, radical pairs and triplet states in photosynthesis. Acc Chem Res 35:313–320

McElroy JD, Feher G, Mauzerall DC (1972) Characterization of primary reactants in bacterial photosynthesis I. Comparison of the light-induced EPR signal ($g = 2.0026$) with that of a bacteriochlorophyll radical. Biochim Biophys Acta 267:363–374

Möbius K, Plato M, Lubitz W (1982) Radicals in solution studied by ENDOR and TRIPLE resonance spectroscopy. Phys Rep 87:171–208

van Mourik F, Reus M, Holzwarth AR (2001) Long-lived charge-separated states in bacterial reaction centers isolated from *Rhodobacter sphaeroides*. Biochim Biophys Acta 1504:311–318

Müh F, Schulz C, Schlodder E, Jones MR, Rautter J, Kuhn M, Lubitz W (1998) Effects of Zwitterionic detergents on the electronic structure of $P^{+}Q_A^{-}$ the primary donor and the charge recombination kinetics of in native and mutant reaction centers from *Rhodobacter sphaeroides*. Photosyn Res 55:199–205

Müh F, Lendzian F, Roy M, Williams JC, Allen JP, Lubitz W (2002) Pigment-protein interactions in bacterial reaction centers and their influence on oxidation potential and spin density distribution of the primary donor. J Phys Chem B 106:3226–3236

Nabedryk E, Schulz C, Müh F, Lubitz W, Breton J (2000) Heterodimeric *versus* homodimeric structure of the primary electron donor in *Rhodobacter sphaeroides* reaction centers genetically modified at position M202. Photochem Photobiol 71:582–588

Norris JR, Uphaus RA, Crespi HL, Katz JJ (1971) Electron spin resonance of chlorophyll and the origin of signal I in photosynthesis. Proc Natl Acad Sci USA 68:625–628

Norris JR, Scheer H, Katz JJ (1975) Models for antenna and reaction center chlorophylls. Ann NY Acad Sci 244:260–280

Plato M, Lubitz W, Möbius K (1981) A solution ENDOR sensitivity study of various nuclei in organic radicals. J Phys Chem 85:1202–1219

Rautter J, Lendzian F, Lubitz W, Wang S, Allen JP (1994) Comparative study of reaction centers from photosynthetic purple bacteria: electron paramagnetic resonance and electron nuclear double resonance spectroscopy. Biochemistry 33:12077–12084

Rautter J, Lendzian F, Schulz C, Fetsch A, Kuhn M, Lin X, Williams JC, Allen JP, Lubitz W (1995) ENDOR studies of the primary donor cation radical in mutant reaction centers of *Rhodobacter sphaeroides* with altered hydrogen-bond interactions. Biochemistry 34:8130–8143

Rautter J, Lendzian F, Lin X, Williams JC, Allen JP, Lubitz W (1996) Effect of orbital asymmetry in $P^{\bullet+}$ on electron transfer in reaction centers of *Rb. sphaeroides*. In: Michel-Beyerle ME (ed) The reaction center of photosynthetic bacteria—structure and dynamics. Springer, Berlin, pp 37–50

Reimers JR, Hush NS (2003) Modeling the bacterial photosynthetic reaction center VII. Full simulation of the intervalence hole-transfer absorption spectrum of the special-pair radical cation. J Chem Phys 119:3262–3277

Reimers JR, Hush NS (2004) A unified description of the electrochemical, charge distribution, and spectroscopic properties of the special-pair radical cation in bacterial photosynthesis. J Am Chem Soc 126:4132–4144

Schulz C, Müh F, Beyer A, Jordan R, Schlodder E, Lubitz W (1998) Investigation of R*hodobacter sphaeroides* reaction center mutants with changed ligands to the primary donor. In: Garab G (ed) Photosynthesis: mechanisms and effects. Kluwer Academic Publishers, Dordrecht, pp 767–770

Sienkiewicz A, Smith BG, Veselov A, Scholes CP (1996) Tunable Q-band resonator for low temperature electron paramagnetic resonance/electron nuclear double resonance measurements. Rev Sci Instrum 67:2134–2138

Silakov A, Reijerse EJ, Albracht SPJ, Hatchikian EC, Lubitz W (2007) The electronic structure of the H-cluster in the [FeFe]-hydrogenase from *Desulfovibrio desulfuricans*: a Q-band ^{57}Fe-ENDOR and HYSCORE study. J Am Chem Soc 129: 11447–11458

Stowell MHB, McPhillips TM, Rees DC, Soltis SM, Abresch E, Feher G (1997) Light-induced structural changes in photosynthetic reaction center: implications for mechanism of electron-proton transfer. Science 276:812–816

Tränkle E, Lendzian F (1989) Computer analysis of spectra with strongly overlapping lines. Application to TRIPLE resonance spectra of the chlorophyll *a* cation radical. J Mag Res 84: 537–547

Williams JC, Allen JP (2008) Directed modification of reaction centers from purple bacteria. In: Thurnauer M, Hunter N, Daldal F (eds) Anoxygenic photosynthetic bacteria II. Springer-Verlag, Dordrecht, pp 337–353

Williams JC, Haffa ALM, McCulley JL, Woodbury NW, Allen JP (2001) Electrostatic interactions between charged amino acid residues and the bacteriochlorophyll dimer in reaction centers from *Rhodobacter sphaeroides*. Biochemistry 40:15403–15407

Yeates TO, Komiya H, Chirino A, Rees DC, Allen JP, Feher G (1988) Structure of the reaction center from *Rhodobacter sphaeroides* R-26 and 2.4.1: protein-cofactor (bacteriochlorophyll, bacteriopheophytin, and carotenoid) interactions. Proc Natl Acad Sci USA 85:7993–7997

Zweygart W, Thanner R, Lubitz W (1994) An improved TM_{110} ENDOR cavity for the investigation of transition metal complexes. J Mag Res A 109:172–176